

1 **Calcite precipitation from CO₂-H₂O-Ca(OH)₂ slurry under**
2 **high pressure of CO₂**

3
4 G. Montes-Hernandez ^{*a, b}, F. Renard ^{a, c}, N. Geoffroy ^a, L. Charlet ^a, J. Pironon ^b

5
6 ^a LGIT, CNRS-OSUG-UJF, Maison de Géosciences, BP 53 X, 38420 Grenoble Cedex 9

7 ^b G2R, Nancy Université, CNRS, BP 239, 54506 Vandoeuvre lès-Nancy, France

8 ^c Physics of Geological Processes, University of Oslo, Norway

9
10 ^{*} Corresponding author: German Montes-Hernandez

11 E-mail address: German.MONTES-HERNANDEZ@obs.ujf-grenoble.fr

12 german_montes@hotmail.com

1 **Abstract**

2

3 The formation of solid calcium carbonate (CaCO_3) from aqueous solutions or slurries
4 containing calcium and carbon dioxide (CO_2) is a complex process of considerable
5 importance in the ecological, geochemical and biological areas. Moreover, the demand for
6 powdered CaCO_3 has increased considerably recently in various fields of industry. The aim of
7 this study was therefore to synthesize fine particles of calcite with controlled morphology by
8 hydrothermal carbonation of calcium hydroxide at high CO_2 pressure (initial P_{CO_2} =55 bar)
9 and at moderate and high temperature (30 and 90°C). The morphology of precipitated
10 particles was identified by transmission electron microscopy (TEM/EDS) and scanning
11 electron microscopy (SEM/EDS). In addition, an X-ray diffraction analysis was performed to
12 investigate the carbonation efficiency and purity of the solid product.

13 Carbonation of dispersed calcium hydroxide ($\text{Ca}(\text{OH})_{2(s)} + \text{CO}_{2(aq)} \rightarrow \text{CaCO}_{3(s)} + \text{H}_2\text{O}$) in the
14 presence of supercritical ($P_T=90$ bar, $T=90^\circ\text{C}$) or gaseous ($P_T=55$ bar, $T=30^\circ\text{C}$) CO_2 led to the
15 precipitation of sub-micrometric isolated particles ($<1\mu\text{m}$) and micrometric agglomerates
16 ($<5\mu\text{m}$) of calcite. For this study, the carbonation efficiency ($\text{Ca}(\text{OH})_2$ - CaCO_3 conversion)
17 was not significantly affected by PT conditions after 24 h of reaction. In contrast, the initial
18 rate of calcium carbonate precipitation increased from 4.3 mol/h in the “90bar- 90°C ” system
19 to 15.9 mol/h in the “55bar- 30°C ” system. The use of high CO_2 pressure may therefore be
20 desirable for increasing the production rate of CaCO_3 , carbonation efficiency and purity, to
21 approximately 48 $\text{kg/m}^3\text{h}$, 95% and 96.3%, respectively in this study. The dissipated heat for
22 this exothermic reaction was estimated by calorimetry to be -32 kJ/mol in the “90bar- 90°C ”
23 system and -42 kJ/mol in the “55bar- 30°C ” system.

24 **Keywords:** A1. Crystal morphology, A1. X-ray diffraction, A2. Hydrothermal crystal
25 growth, B1. Nanomaterials, B1. Minerals

1 **1. Introduction**

2

3 Calcium carbonate is an abundant mineral comprising approximately 4% of the Earth's crust.

4 As an inorganic mineral it is widely used both by man for industrial applications and more

5 generally by living organisms during their development. The carbon dioxide balance in the

6 atmosphere (an integral component of the carbon cycle) is partially controlled through the

7 equilibrium cycling between mineralised calcium carbonate and atmospheric carbon dioxide

8 [1]. The formation of solid calcium carbonate (CaCO_3) from aqueous solutions or slurries

9 containing calcium and carbon dioxide (CO_2) is a complex process of considerable

10 importance in the ecological, geochemical and biological areas. Moreover, the demand for

11 powdered CaCO_3 has increased considerably recently in various fields of industry: paper,

12 paint, magnetic recording, textiles, detergents, adhesives, plastics, cosmetics, food, etc. [2].

13 Calcium carbonate particles have three crystal morphologies, which are generally classified as

14 rhombic calcite, needle-like aragonite and spherical vaterite. Calcite belonging to the

15 Trigonal-Hexagonal-Scaleno-hedral Class is the most stable phase at room temperature under

16 normal atmospheric conditions, while aragonite and vaterite belong to the Orthorombic-

17 Dipyramidal and Hexagonal-Dihexagonal Dipyramidal Classes, respectively. They are

18 metastable polymorphs that readily transform into the stable calcite phase. The polymorphs of

19 crystalline calcium carbonate particles depend mainly on precipitation conditions such as pH,

20 temperature and supersaturation. This last parameter is considered to be the most important

21 controlling factor [3].

22 Many experimental studies have reported the synthetic precipitation of the various forms of

23 calcium carbonate. The conditions under which precipitation may be produced, including the

24 importance of initial supersaturation, temperature, pH, hydrodynamics and the presence of

25 impurities and additives, are well known (see for ex. [4-17]). In general, calcite in a

1 supersaturated solution can be precipitated by nucleation in an early stage and subsequent
2 crystal growth in later stages. Nucleation corresponds to the formation of nuclei or critical
3 clusters where crystal growth can occur spontaneously [18-19]. The structure of these nuclei
4 is not known and is too small to be observed directly.

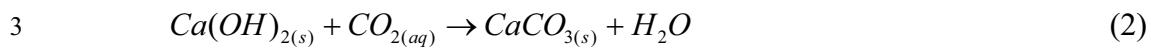
5 The degree of supersaturation (S_I) with respect to calcite is defined as:

$$6 \quad S_I = \frac{(Ca^{2+})(CO_3^{2-})}{K_{sp}} \quad (1)$$

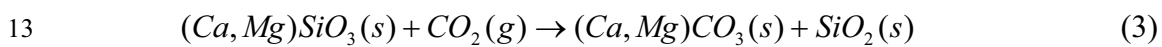
7 where (Ca^{2+}) and (CO_3^{2-}) are the activities of calcium and carbonate ions in the solution,
8 respectively, and K_{sp} is the thermodynamic solubility product of calcite. It is generally
9 agreed that heterogeneous nucleation can be initiated at a lower degree of supersaturation than
10 homogeneous nucleation and different seed crystals will lower the activation energy barrier,
11 depending on the level of molecular recognition between the seed crystal and the precipitating
12 solid phase [18].

13 The low viscosity and high diffusivity of CO_2 occurring in near-critical or supercritical (SC-)
14 state result in enhanced reaction rates for processes carried out involving these media.
15 Therefore, compressed CO_2 has many properties that make it an attractive solvent for
16 industrial chemical processes and/or reactions. SC- CO_2 has been used in a number of
17 industrial processes, most notably as an extraction solvent and for pharmaceutical particle
18 engineering [20]. Promising applications in low-cost bulk materials, such as cement, are also
19 being widely investigated in order to improve concrete strength for immobilizing radioactive
20 waste [21, 22]. There has also been a general recent trend in the chemical and petrochemical
21 industry to operate gas absorption units at high pressure for both technical and economic
22 reasons. Recently, the precipitation of calcium carbonate in compressed and supercritical CO_2
23 was proposed as an innovative method for producing calcite by aqueous-carbonation with
24 potential benefits for industrial applications [2, 23]. Note that, for these applications, SC- CO_2

1 is not used as a solvent but as a reagent for calcite precipitation. See for example, the
2 following overall reaction:



4 Finally, the increasing CO₂ concentration in the earth's atmosphere, mainly caused by fossil
5 fuel combustion, has led to concerns about global warming. A technology that could possibly
6 contribute to reducing carbon dioxide emissions is the in situ sequestration (geological
7 storage) or ex-situ sequestration (controlled reactors) of CO₂ by mineral carbonation, as
8 originally proposed by Seifritz [24] and first studied in detail by Lackner et al. [25]. At the
9 present time, several theoretical and/or experimental studies on CO₂ sequestration have been
10 reported in the literature (see for example [26-45]). The basic concept behind mineral CO₂
11 sequestration is to mimic natural weathering processes in which calcium or magnesium
12 silicates are transformed into carbonates:



14 The aim of this study was to synthesize fine particles of calcite with controlled morphology
15 by using hydrothermal carbonation of calcium hydroxide at high CO₂ pressure (initial
16 P_{CO₂}=55 bar) and at moderate and high temperature (30, 90°C). In addition, a simplified
17 method was proposed to estimate the calcium carbonate production rate, carbonation
18 efficiency, purity and dissipated heat of the exothermic reaction.

19 Portlandite Ca(OH)₂ material was chosen because this mineral is an important component in
20 cement to be used in concrete injection systems for geological storage of CO₂. Here, cement
21 carbonation is the main chemical transformation occurring in borehole materials in contact
22 with CO₂. This process could be the cause of a possible loss of borehole integrity, inducing
23 leakage of the gas to the surface. In addition, the carbonation of Ca(OH)₂ at high CO₂
24 pressure was recently proposed as a novel method to produce fine particles of calcite [2, 23].

25 **2. Materials and methods**

1

2 2.1 Carbonation of calcium hydroxide (stirred reactor)

3 One litre of high-purity water with electrical resistivity of 18.2 MΩ cm and 74.1g of
4 commercial calcium hydroxide (provided by Sigma-Aldrich) with 96% chemical purity (3%
5 CaCO₃ and 1% other impurities) were placed in a titanium reactor (autoclave with internal
6 volume of two litres). The hydroxide particles were immediately dispersed with mechanical
7 agitation (400 rpm). The dispersion was then heated to 90°C with a heating system adapted to
8 the reactor. When the dispersion temperature was reached, 80.18 g of CO₂ (provided by Linde
9 Gas S.A.) were injected in the reactor and the total pressure in the system was immediately
10 adjusted to 90 bar by argon injection (see Fig. 1). Under these T and P conditions, the vapour
11 phase consists mainly of an Ar+CO₂ mixture with the CO₂ in a supercritical state. In order to
12 evaluate the precipitation (or production) rate, four different reaction durations were
13 considered (0.25, 0.5, 4 and 24 h). The experiments were also carried out at 30°C and 55 bar
14 for reaction durations of 0.25, 4 and 24 h. For this second case, 96.05 g of CO₂ were initially
15 injected in the reactor. At 55 bar and 30°C, the vapour phase consists mainly of gaseous CO₂.
16 At the end of the experiment, the autoclave was removed from heating system and immersed
17 in cold water. The reaction cell was depressurized during the water cooling period. After
18 water cooling at 35°C (about 15 minutes) the autoclave was disassembled, and the solid
19 product was carefully recovered and separated by centrifugation (30 minutes at 12,000 rpm),
20 decanting the supernatant solutions. Finally, the solid product was dried directly in the
21 centrifugation flasks for 48 h at 60°C and consecutively for 12 h at 110°C in order to
22 eliminate the adsorbed water. The weight of dry solid product was then calculated by the
23 following simple mass balance:

$$24 \quad W_{dry_product} = W_{flask+dry_product} - W_{flask} \quad (4)$$

1 Note that the reaction cell was depressurized immediately after immersion in cold water. In
2 order to evaluate the effect of the depressurization stage on the final product composition, a
3 test experiment was performed at 90 bar and 90°C for a reaction time of 4 h. In this case, the
4 reactor was depressurized after water cooling at 35°C, for 45 minutes.

5

6 2.2 Characterization of solid phase

7 Morphological analyses of the solid products were performed using a Hitachi 22500 Fevex
8 scanning electron microscope. Isolated fine particles (oriented on carbon Ni-grids) of the
9 starting material and product were also studied using a Jeol 3010 transmission electron
10 microscope, equipped with an energy dispersive X-ray analyser (EDS) to illustrate particle
11 morphology and to identify the precipitated phases. The starting material and solid products
12 were also characterized by X-ray powder diffraction using a Siemens D501 diffractometer
13 with a θ , 2θ geometry. The XRD patterns were recorded in the $5-80^\circ 2\theta$ range using Cok α
14 radiation ($\lambda=1.7902 \text{ \AA}$). The experimental measurement parameters were 8s counting time per
15 $0.02^\circ 2\theta$ step. A Kevex Si(Li) detector is used for this purpose.

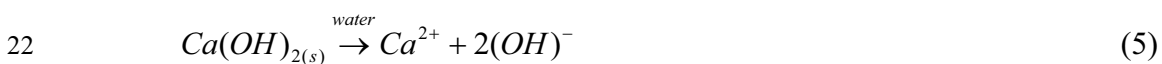
16

17 3. Results and discussion

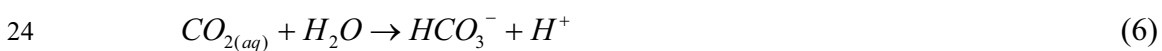
18

19 3.1 Dissipated heat of Ca(OH)₂ carbonation

20 The aqueous carbonation of calcium hydroxide described by the global reaction (2) is an
21 exothermic process which concerns simultaneously the dissolution of calcium hydroxide,



23 and the dissociation of aqueous CO₂,



1 Therefore, the dissipated heat (q) for the overall calcium hydroxide carbonation process
2 (reaction (2)) can be calculated by using the calorimetry concept:

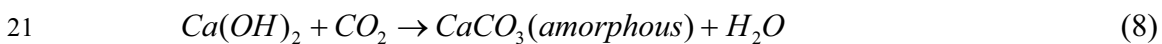
$$3 \quad q = (m)(c)(\Delta T) \quad (7)$$

4 where m is the mass of water in the reactor (1000 g), c is the specific heat of water (4.19
5 J/g°C) and ΔT is the change in water temperature. The temperature change was directly
6 monitored in the reactor as a function of time for each experiment (see for ex. Fig. 2 and
7 Table 1). The average value of ΔT was estimated to be 7.5°C ($\pm 1^\circ\text{C}$) for the 90bar-90°C
8 system and 10°C ($\pm 1^\circ\text{C}$) for the 55bar-30°C system. This significant variation in ΔT could be
9 due to the quantity of CO₂ dissolved in the aqueous solution because the solubility of CO₂
10 decreases significantly with increase in temperature. In contrast, CO₂ solubility increases
11 slightly with increase in pressure (see for ex. [46-47]). Considering the quantity of Ca(OH)₂
12 used in the reaction (74.1 g), the dissipated heats for this exothermic process were -31.4
13 kJ/mol and -41.9 kJ/mol, respectively.

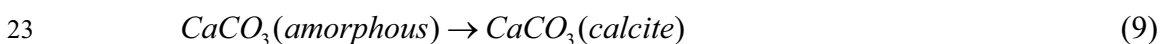
14

15 3.2 Carbonation efficiency and purity

16 The X-ray spectra in Fig. 3 show the qualitative variation in carbonation for the 90bar-90°C
17 and 55bar-30°C systems at different reaction times. Note the high rate of carbonation process
18 and high purity of precipitated calcite. These results suggest a simple mechanism for calcite
19 precipitation, first spontaneous precipitation of amorphous calcium carbonate and then calcite
20 formation. This process can be represented by the following successive chemical reactions:



22 and,



24 The metastable crystalline phases of calcium carbonate, such as vaterite and aragonite, were
25 not identified during the calcium hydroxide carbonation process, except in the test

1 experiment, i.e. when the reactor was depressurized after the water cooling stage at 35°C. For
 2 this case, crystalline aragonite was also identified by X-ray diffraction (see Fig. 4).
 3 Obviously, this crystalline phase was formed during water cooling stage, but the
 4 physicochemical mechanism is not clear. The excess CO₂ in the system (about 0.9 mol) may
 5 play a significant role in this unusual process, possibly with partial dissolution of calcite
 6 particles and then aragonite precipitation and calcium hydroxide re-crystallization during
 7 reactor depressurization at low temperature.

8 For this study, the presence of supercritical CO₂ did not have a clear effect on the Ca(OH)₂
 9 carbonation process. This confirms the low reactivity of molecular CO₂ on calcite dissolution
 10 [44] and precipitation (this study). In contrast, the temperature of reaction has a significant
 11 effect on carbonation rate (see Figure 2). In fact, the precipitation rate is proportional to the
 12 quantity of dissolved CO₂. This justifies a higher rate of carbonation at low temperature.

13 From the qualitative characterization by X-ray diffraction discussed above the carbonation
 14 efficiency and chemical purity of calcium carbonate were calculated using a mass balance
 15 method, based on the theoretical overall carbonation reaction (see Table 2). The carbonation
 16 efficiency (*CE*) was then calculated by the following equation:

$$17 \quad CE = \frac{w_{dry_product} - w_{Ca(OH)2(initial)}}{w_{theoretical} - w_{Ca(OH)2(initial)}} * 100 \quad (10)$$

18 where $w_{dry_product}$ is the experimental mass of solid product [g] (see Eq. 4), $w_{theoretical}$ is the
 19 theoretical mass of calcium carbonate calculated by using Eq. (2) [g] and considering 100%
 20 of carbonation (Ca(OH)₂-CaCO₃ transformation), $w_{Ca(OH)2(initial)}$ is the initial mass of calcium
 21 hydroxide charged into the reactor [g]. Consequently, the non-reacted calcium hydroxide in
 22 the solid product [g] was calculated by:

$$23 \quad w_{Ca(OH)2(non-reacted)} = w_{Ca(OH)2(initial)} - w_{Ca(OH)2(initial)} * CE \quad (11)$$

1 Then, the precipitated quantity of calcium carbonate [g] was calculated by a simple mass
2 balance:

$$3 \quad W_{CaCO3(precipitated)} = W_{dry_product} - W_{Ca(OH)2(non-reacted)} \quad (12)$$

4 Finally, the purity of calcium carbonate was calculated by:

$$5 \quad Purity = \frac{W_{CaCO3(precipitated)}}{W_{CaCO3(precipitated)} + W_{Ca(OH)2(non-reacted)}} * 100 \quad (13)$$

6 All the values are given in Table 2. Note that carbonation efficiency quickly exceeds 90% and
7 reaches a maximum of about 95%. Consequently, the maximum purity value of 96.3% was
8 calculated. The carbonation efficiency and purity of the product obtained by the proposed
9 method could have advantageous technological and environmental applications because it is
10 well-known that the traditional industrial method for carbonation by CO₂ bubbling gives
11 lower precipitation efficiencies (see for ex. [2, 23]).

12 The carbonation of dispersed calcium hydroxide (Eq. 2) in presence of supercritical or
13 gaseous CO₂ led to the precipitation of sub-micrometric isolated particles (<1 μm) and
14 micrometric agglomerates (<5 μm) of calcite (see Figure 5).

15

16 3.3 Fitting of kinetic experimental data

17 Several kinetic models including first-order, pseudo-first-order, second-order, pseudo-second-
18 order, parabolic diffusion and power function kinetic expressions are reported in the literature
19 for fitting the kinetic experimental data of a solid-liquid separation process. For this study, the
20 kinetic experimental data concern calcium carbonate precipitation; in this case, the best fit
21 (attested by a correlation factor close to 1) of the experimental data was achieved when using
22 a pseudo-second-order kinetic model according to the following expression:

$$23 \quad \frac{d[Mol_{CaCO3,t}]}{dt} = k_p (Mol_{CaCO3,max} - Mol_{CaCO3,t})^2 \quad (14)$$

1 where k_p is the rate constant of calcite precipitation [1/mol h] for a given initial dose of
 2 Ca(OH)_2 , $Mol_{\text{CaCO}_3, \text{max}}$ is the maximum precipitated quantity of calcium carbonate at
 3 equilibrium [mol], $Mol_{\text{CaCO}_3, t}$ is the precipitated quantity of calcium carbonate at any time, t ,
 4 [mol].

5 The integrated form of Equation (14) for the boundary conditions $t = 0$ to $t = t$ and $Mol_{\text{CaCO}_3, t}$
 6 $= 0$ to $Mol_{\text{CaCO}_3, t} = Mol_{\text{CaCO}_3, t}$, is represented by a hyperbolic equation:

$$7 \quad Mol_{\text{CaCO}_3, t} = \frac{Mol_{\text{CaCO}_3, \text{max}} * t}{\left(\frac{1}{k_p * Mol_{\text{CaCO}_3, \text{max}}} \right) + t} \quad (15)$$

8 In order to simplify the experimental data, fitting a novel constant can be defined
 9 “ $(1/k_p * Mol_{\text{CaCO}_3, \text{max}}) = t_{1/2}$ ”. Physically, this constant represents the time after which half of the
 10 maximum precipitated quantity of calcium carbonate was obtained. In the current study, $t_{1/2}$ is
 11 called “half-precipitation time” and can be used to calculate the initial rate of calcium
 12 carbonate precipitation, $v_{0,p}$, [mol/h] by the following expression:

$$13 \quad v_{0,p} = \frac{Mol_{\text{CaCO}_3, \text{max}}}{t_{1/2}} = k_p (Mol_{\text{CaCO}_3, \text{max}})^2 \quad (16)$$

14 The fitting of experimental kinetic curves ($Mol_{\text{CaCO}_3, t}$ vs. t) using Equation (15) is shown in
 15 Figure 6. The parameters $t_{1/2}$ and $Mol_{\text{CaCO}_3, \text{max}}$ were estimated by applying non-linear
 16 regression by the least squares method.

17 Finally, based on the initial rate of calcium carbonate precipitation the optimum production
 18 rate, P_{rate} [kg/m³h] of calcium carbonate can be calculated for a given dose of calcium
 19 hydroxide using the following expression:

$$20 \quad P_{\text{rate}} = \frac{Mol_{\text{CaCO}_3, \text{max}} * M_{\text{CaCO}_3}}{t_{1/2} * V_{\text{reactor}}} \quad (17)$$

21 where M_{CaCO_3} is the molar mass of calcium carbonate and V_{reactor} is the effective volume of
 22 the reactor, (2L) for this study.

1 The calculations using Eq. (17) show that the calcium carbonate production rate in the 55bar-
2 30°C system ($798.6 \text{ kg/m}^3\text{h}$, $v_{0,p}=15.9 \text{ mol/h}$) is higher than the production rate in the 90bar-
3 90°C system ($213.17 \text{ kg/m}^3\text{h}$, $v_{0,p}=4.3 \text{ mol/h}$). This confirms the qualitative observations
4 discussed above. It is important to note that the initial rate of calcium carbonate precipitation,
5 and consequently the production rate calculation, depends only on the $t_{1/2}$ parameter, which in
6 turn depends on the PT conditions.

7 Note that the production rate was calculated using the $t_{1/2}$ parameter. Obviously, this is an
8 ideal calculation. A more realistic calculation could be suggested based on the experiments
9 and solid product characterization using a 1h reaction time for both the systems studied in
10 order to obtain better product maturity. In this case, the average production rate is estimated
11 to be $47.94 \text{ kg/m}^3\text{h}$.

12

13 **4. Conclusion**

14

15 In conclusion, the results of this research show that the carbonation of dispersed calcium
16 hydroxide in water with co-existence of supercritical or gaseous CO_2 leads to the precipitation
17 of sub-micrometric isolated particles ($<1 \mu\text{m}$) and micrometric agglomerates ($<5 \mu\text{m}$) of
18 calcite. In this study, the carbonation efficiency ($\text{Ca(OH)}_2\text{-CaCO}_3$ conversion) is not
19 significantly affected by PT conditions after 24 h of reaction. In contrast, the initial rate of
20 calcium carbonate precipitation increases from 4.3 mol/h in the “90bar-90°C” system to 15.9
21 mol/h in the “55bar-30°C” system. The use of high CO_2 pressure (initial $P_{\text{CO}_2}=55 \text{ bar}$) could
22 represent an improvement for increasing the CaCO_3 production rate, carbonation efficiency and
23 purity, which were respectively equal to $48 \text{ kg/m}^3\text{h}$, 95% and 96.3% in this study. The
24 dissipated heat for this exothermic reaction was estimated by calorimetry concept, -32 kJ/mol
25 for the “90bar-90°C” system and -42 kJ/mol for the “55bar-30°C” system. The results

1 presented here suggest that the carbonation of calcium hydroxide in presence of supercritical
2 or gaseous CO₂ could be a powerful technique for producing fine-particles of calcite on an
3 industrial scale. This research also has important ecological implications for the ex-situ
4 mineral sequestration of CO₂ by alkaline liquid-solid waste (ex. fly ash, bottom ash, Ca/Mg-
5 rich silicates, alkaline waste water, etc.).

6

1 **Acknowledgements**

2

3 The authors are grateful to the National Research Agency, ANR (GeoCarbone-
4 CARBONATATION and INTEGRITY projects) and the National Research Council (CNRS),
5 France, for providing a financial support for this work. This study has also been financed
6 through collaboration between the University of Grenoble (German Montes-Hernandez,
7 François Renard) and Gaz de France (Christophe Rigollet, Samuel SAYSSET, Rémi Dreux).

8

1 **References**

2

3 [1] Dickinson, S. R.; Henderson, G. E.; McGrath, K. M., *J. Crystal Growth* 244 (2002) 369.

4 [2] Domingo, C.; Loste, E.; Gomez-Morales, J.; Garcia-Carmona, J.; Fraile, J., *The Journal of*
5 *Supercritical Fluids* 36 (2006) 202.

6 [3] Han, Y. S.; Hadiko, G.; Fuji, M.; Takahashi, M., *J. Crystal Growth* 276 (2005) 541.

7 [4] Moore, L.; Hopwood, J D.; Davey, R. J., *J. Crystal Growth* 261 (2004) 93.

8 [5] Westin, K. J., Rasmuson, A. C., *Journal of Colloids and Interface Science* 282 (2005) 370.

9 [6] Tsuno, H., Kagi, H., Akagi T., *Bull. Chem. Soc. Jpn.* 74 (2001) 479.

10 [7] Fujita, Y., Redden, G. D., Ingram, J., Cortez, M. M., Ferris, G., Smith, R. W., *Geochimica*
11 *et Cosmochimica Acta* 68/15 (2004) 3261.

12 [8] Freij, S. J., Godelitsas, A., Putnis, A., *J. Crystal Growth* 273 (2005) 535.

13 [9] Gower, L. A., Tirrell, D. A., *J. Crystal Growth* 191 (1998) 153.

14 [10] Jonasson, R. G., Rispler, K., Wiwchar, B., Gunter, W. D., *Chemical Geology* 132 (1996)
15 215.

16 [11] Chrissanthopoulos, A., Tzanetos, N. P., Andreopoulou, A. K., Kallitsis, J., Dalas, E., *J.*
17 *Crystal Growth* 280 (2005) 594.

18 [12] Menadakis, M., Maroulis, G., Koutsoukos, P. G., *Computational Materials Science* 38
19 (2007) 522.

20 [13] Dousi, E., Kallitsis, J., Chrissanthopoulos, A., Mangood, A. H., Dalas, E., *J. Crystal*
21 *Growth* 253 (2003) 496.

22 [14] Pastero, L., Costa, E., Alessandria, B., Rubbo, M., Aquilano, D., *J. Crystal Growth* 247
23 (2003) 472.

24 [15] Lee, Y. J., Reeder, R., *Geochemica et Cosmochemica Acta* 70 (2006) 2253.

- 1 [16] Temmam, M., Paquette, J., Vali, H., *Geochemica et Cosmochemica Acta* 64/14 (2000)
2 2417.
- 3 [17] Dalas, E., Chalias, A., Gatos, D., Barlos, K., *Journal of Colloids and Interface Science*
4 300 (2006) 536.
- 5 [18] Stumm, W. and Morgan J. J., *Aquatic Chemistry* (1996) Wiley-Interscience
- 6 [19] Lin, Y. P. and Singer P. C., *Geochimica et Cosmochimica Acta* 69/18 (2005) 4495.
- 7 [20] McHugh, M. and Krukoniš V. *Supercritical Fluid Extraction: Principles and Practices*
8 (1994) Butterworth-Heineman, US.
- 9 [21] Jones, R. H. (1999) US Patent 5, 965, 201.
- 10 [22] Ginneken; L. V.; Dutré, V. Adriansens W., Weyten H., *The Journal of Supercritical*
11 *Fluids* 30/02 (2004)175.
- 12 [23] Domingo, C.; Garcia-Carmona, J.; Loste, E.; Fanovich, A.; Fraile, J. Gomez-Morales J.,
13 *J. Crystal Growth* 271 (2004) 268.
- 14 [24] Seifritz, W., *Nature* 345 (1990) 486.
- 15 [25] Lackner, K. S.; Wendt, C. H.; Butt, D. P.; Joyce, E. L.; Sharp, D. H., *Energy* 20/11
16 (1995) 1153.
- 17 [26] Knauss, K. G.; Johnson, J. W.; Steefel, C. I., *Chemical Geology* 217 (2005) 339.
- 18 [27] Pruess, K. T.; Xu, J.; Apps, J.; García, *SPE Journal* (2003) 49.
- 19 [28] Bachu, S., *Energy Convers Mgmt.* 43 (2002) 87.
- 20 [29] Huijgen, W. J. J.; Witkamp, G-J.; Comans R. N. J., *Environmental Science and*
21 *Technology* (2005) 9676.
- 22 [30] Rosenbauer, R. J.; Koksalan, T.; Palandri J. L., *Fuel Processing Technology* 86 (2005)
23 1581.
- 24 [31] Kaszuba, J. P.; Janecky, D. R.; Snow, M. G., *Chemical Geology* 217 (2005) 277.
- 25 [32] Kaszuba, J. P.; Janecky, D. R.; Snow, M. G., *Applied Geochemistry* 18 (2003) 1065.

- 1 [33] Palandri, J. L.; Rosenbauer, R. J.; Kharaka, Y. K., *Applied Geochemistry* 20 (2005)
2 2038.
- 3 [34] Giammar, D. E.; Bruant Jr., R. G.; Poters, C. A., *Chemical Geology* 217 (2005) 257.
- 4 [35] Gunter, W. D.; Perkins, E. H.; Hutcheon I., *Applied Geochemistry* 15 (2000) 1085.
- 5 [36] Okamoto, I.; Li, X.; Ohsumi, T., *Energy* 30 (2005) 2344.
- 6 [37] Park, A-H. A.; Fan, L-S., *Chemical Engineering Science* 59 (2004) 5241.
- 7 [38] Rendek, E.; Ducom, G.; Germain, P., *Journal of Hazardous Materials B*128 (2006) 73.
- 8 [39] Meima, J. A.; Van der Weijden, D.; Eighmy, T. T.; Comans, R. N. J., *Applied*
9 *Geochemistry* 17 (2002) 1503.
- 10 [40] Regnault, O.; Lagneau, V.; Catalette, H.; Schneider, H., *Comptes Rendus Geoscience.*
11 (2005) 1331.
- 12 [41] Xu, T.; Apps, J. A.; Pruess, K., *Chemical Geology* 217 (2005) 295.
- 13 [42] Bachu, S.; Adams, J. J., *Energy Conversion and Management* 44 (2003) 3151.
- 14 [43] White, S. P.; Allis, R. G.; Moore, J.; Chidsey, T.; Morgan, C.; Gwynn, W.; Adams, M.,
15 *Chemical Geology* 217 (2005) 387.
- 16 [44] Pokrovsky, O. S., Gobulev, S. V., Schott, J., *Chemical Geology* 217 (2005) 239.
- 17 [45] Le Guen, Y., Renard, F., Hellmann, R., Collombet, M., Tisserand, D., Brosse, E.,
18 Gratier, J. P., *Journal of Geophysical Research* 112 (2007) B05421.
- 19 [46] Duan, Z., Sun, R., *Chemical Geology* 193 (2003) 257.
- 20 [47] Duan, Z., Sun, R., Zhu, C., Chou, I.-M., *Mar. Chem.* 98 (2006) 131.
- 21

1 Table 1. Average ΔT calculation for “90bar-90°C” and “55bar-30°C” systems

Experiment	$T_{initial}$	$T_{maximal}$	$\Delta T = T_{maximal} - T_{initial}$
90bar-90°C system			
0.25h	90	97	7
0.50h	90	98	8
4h	90	98	8
24h	90	97	7
			$\overline{\Delta T} = 7.5$
55bar-30°C system			
0.25h	30	40	10
4h	30	41	11
24h	30	40	10
			$\overline{\Delta T} = 10.33 \cong 10$

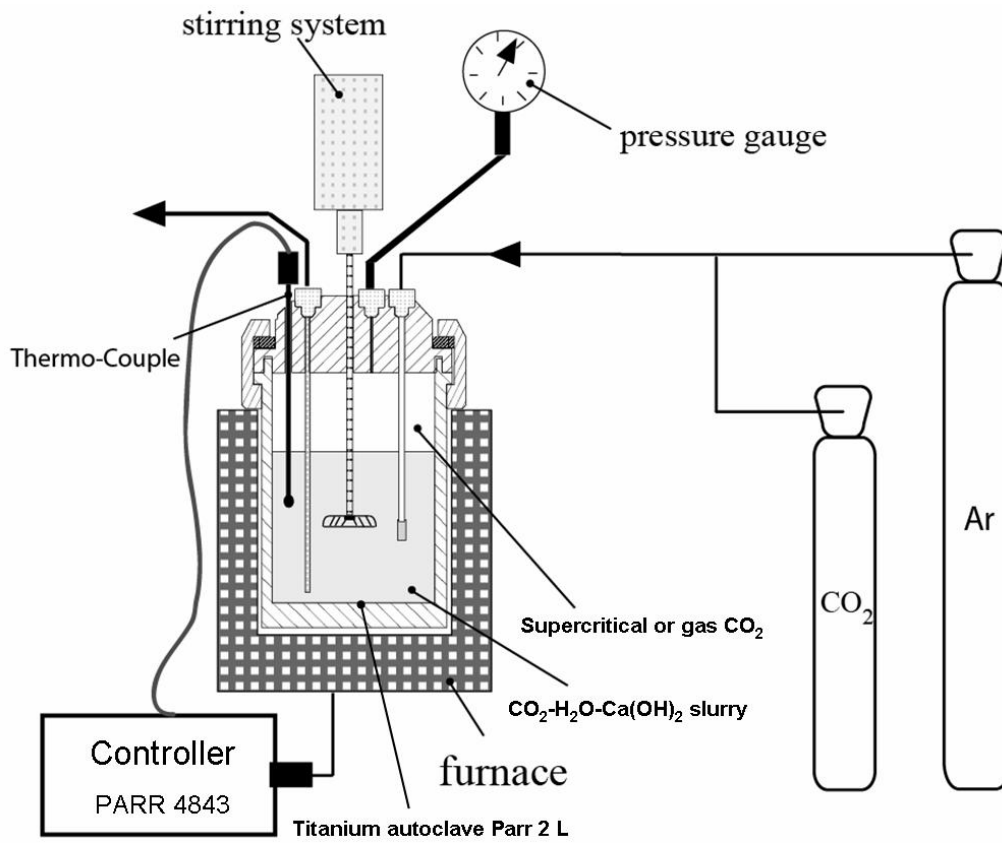
- 2 $T_{initial}$ is the initial temperature before the carbonation reaction
3 $T_{maximal}$ is the maximum temperature reached during the carbonation reaction
4 ΔT is the change in water temperature during the carbonation reaction
5

- 1 Table 2. Carbonation efficiency (*CE*) and chemical purity calculations for 90bar-90°C and
 2 55bar-30°C systems using a mass balance method.

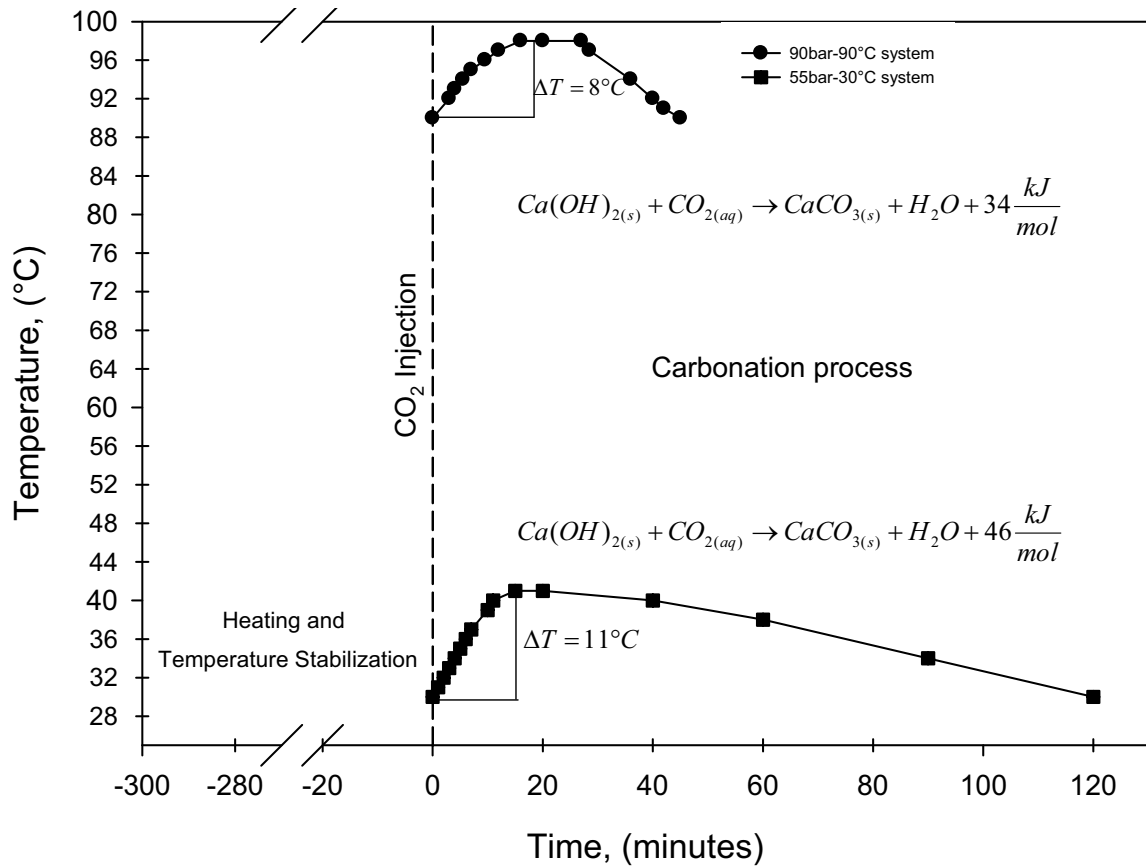
Time, [h]	$w_{dry_product}$ [g]	<i>CE</i> [%]	$w_{CaCO3(precipitated)}$ [g]	$w_{Ca(OH)2(non-reacted)}$ [g]	Purity* [%]
90bar-90°C system					
0.25	85.34	43.3	43.3	42.0	50.7
0.50	93.42	74.3	74.4	19.0	79.7
4	97.91	91.6	91.7	6.2	93.7
24	98.04	92.1	92.2	5.8	94.0
55bar-30°C system					
0.25	94.22	77.4	77.5	16.7	82.3
4	98.80	95.0	95.1	3.6	96.3
24	98.75	94.9	94.9	3.8	96.2

- 3 * Taking into account only two solid phases ($CaCO_3$ and $Ca(OH)_2$)

4



1
 2 Figure 1. Schematic experimental system for calcite precipitation from CO₂-H₂O-Ca(OH)₂
 3 slurry in presence of supercritical (90 bar and 90°C) and gaseous (55 bar and 30°C) CO₂.



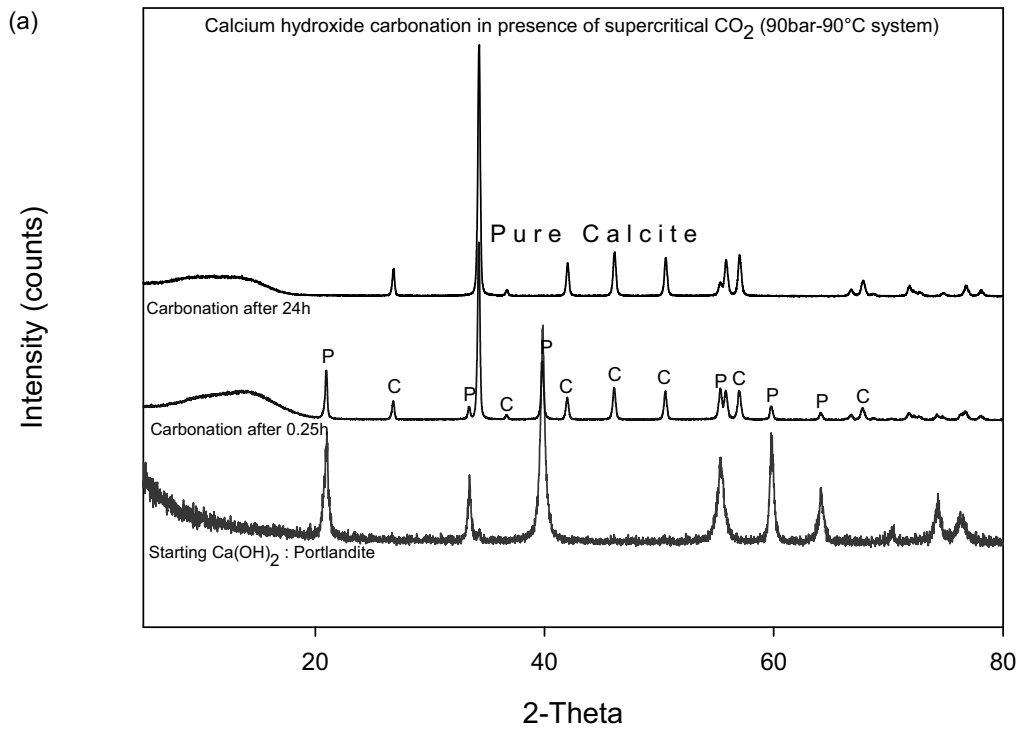
1

2 Figure 2. Temperature variation during calcite precipitation for “90bar-90°C” and “55bar-

3 30°C” systems. Estimation of ΔT (temperature change) and calculation of dissipated heat.

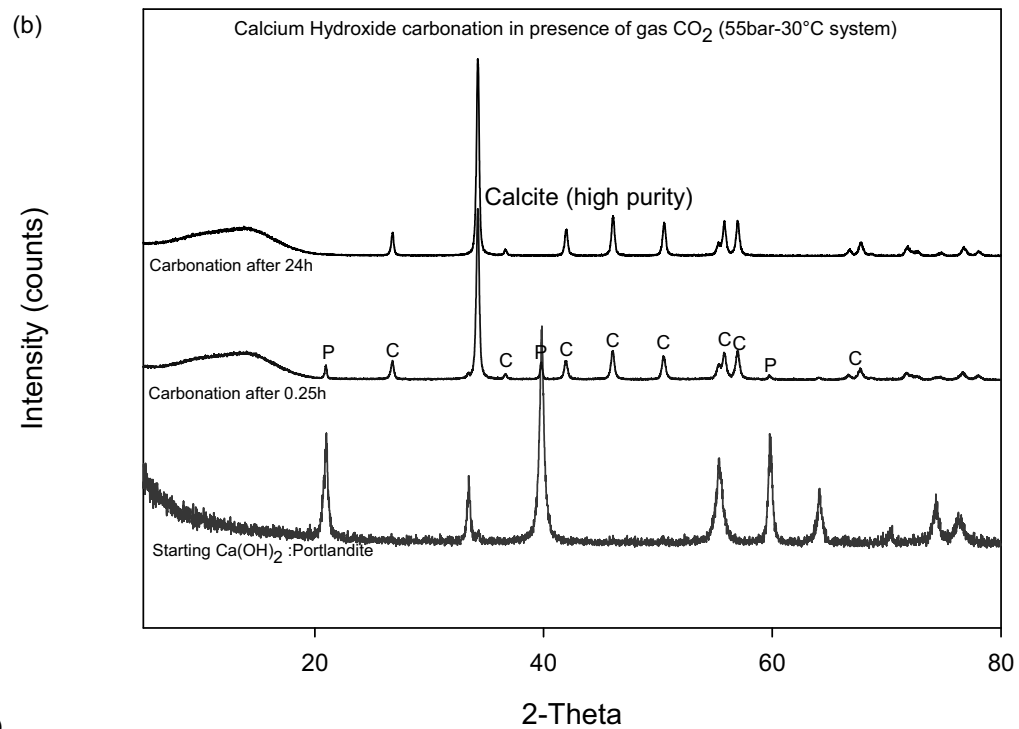
4

5



1

a)



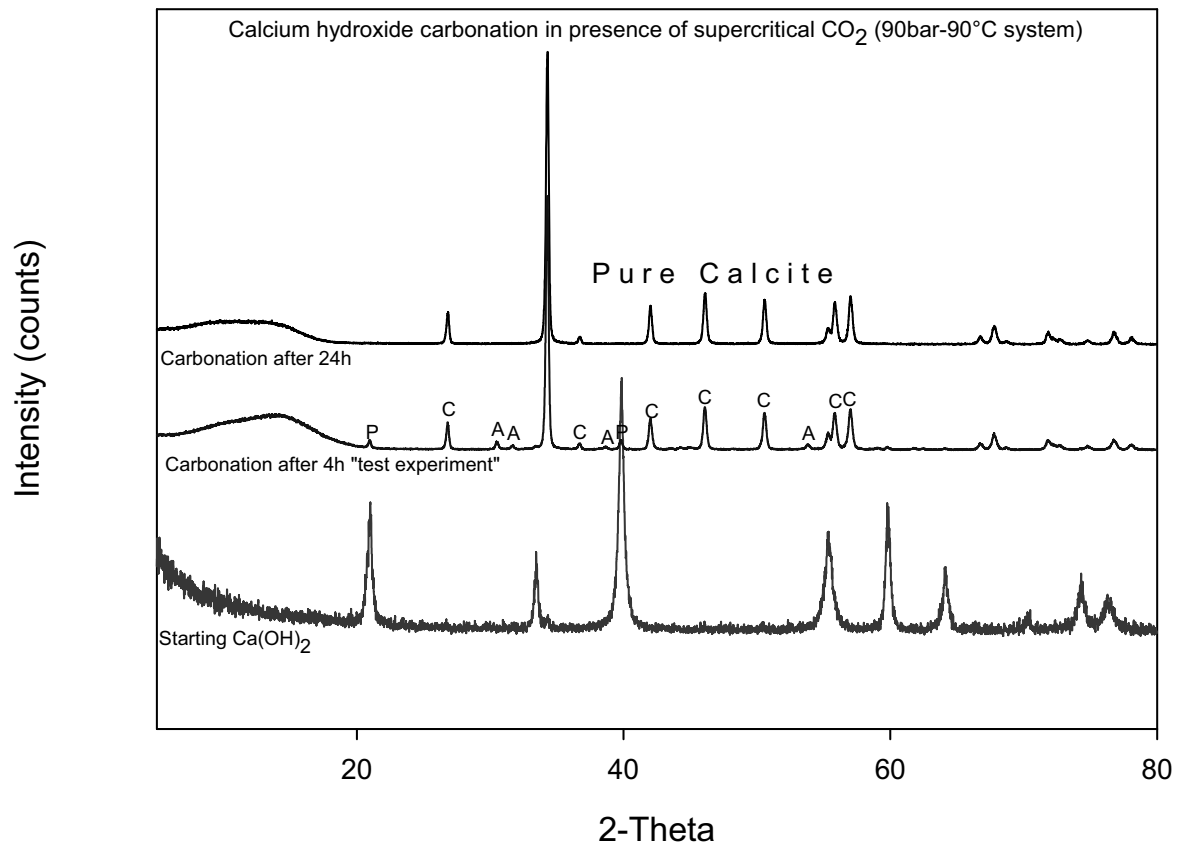
2

b)

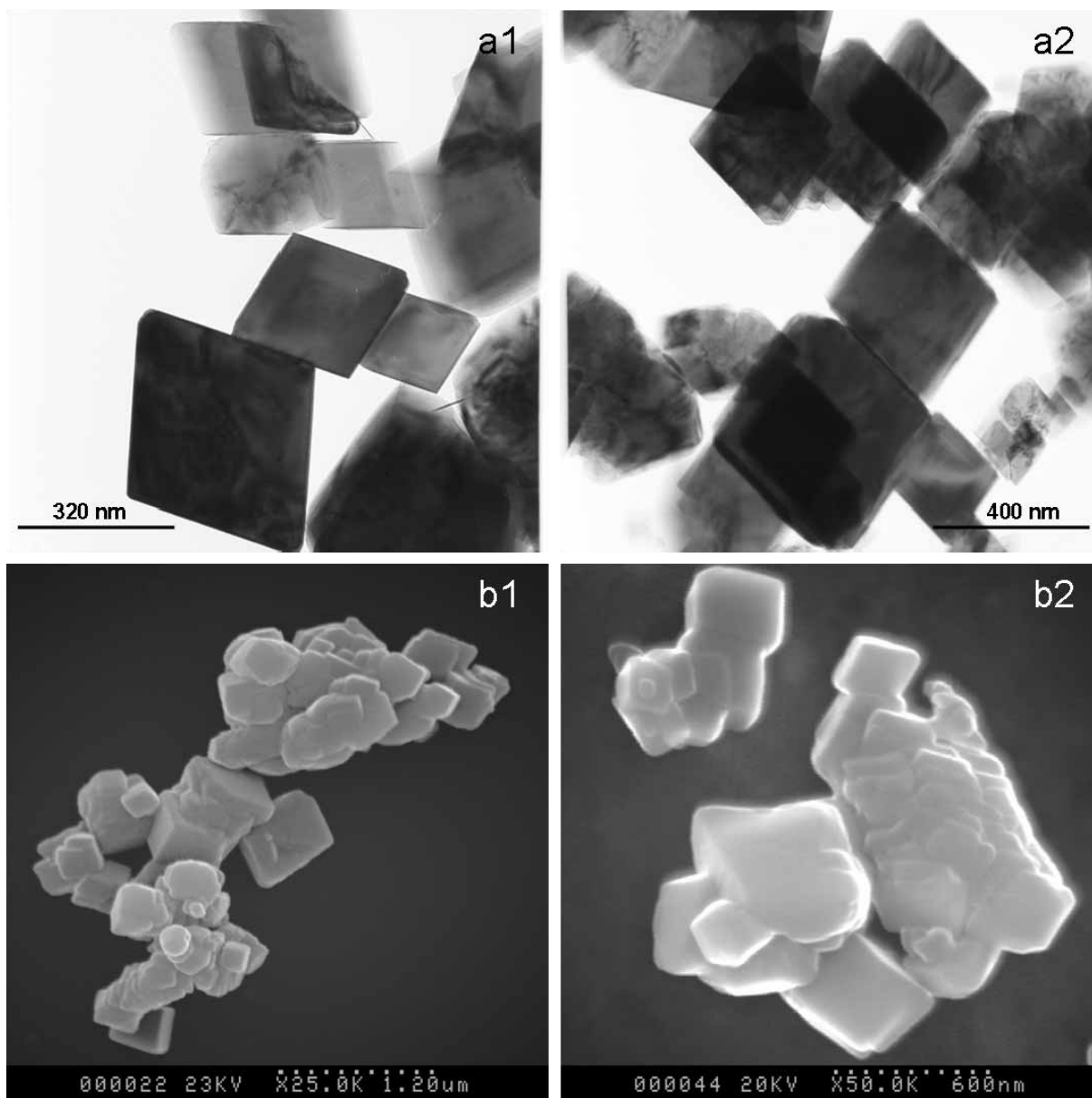
3 Figure 3. XRD measurements of initial calcium hydroxide and solid products. (a) Ca(OH)₂
 4 carbonation in presence of supercritical CO₂ and (b) gaseous CO₂ at different reaction
 5 times of. P: Portlandite, C: Calcite.

6

7



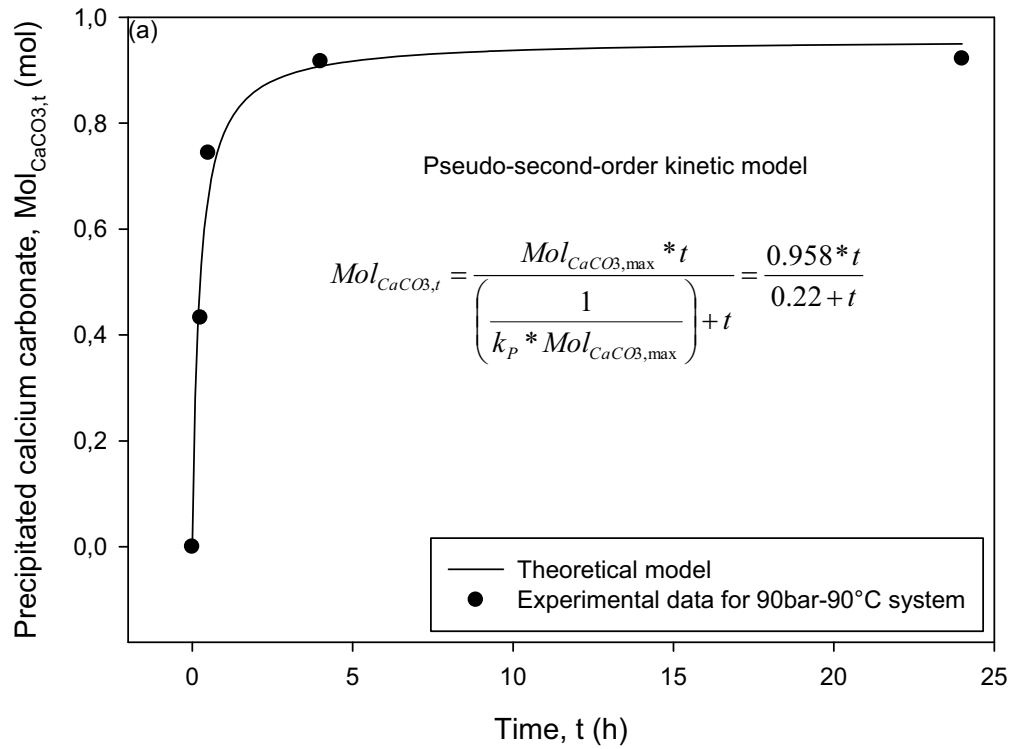
- 1
- 2 Figure 4. Test experiment “depressurization stage of reactor after water cooling at 35°C”.
- 3 Formation of the crystalline aragonite during the water cooling stage. P: Portlandite, C:
- 4 Calcite, A:Aragonite.



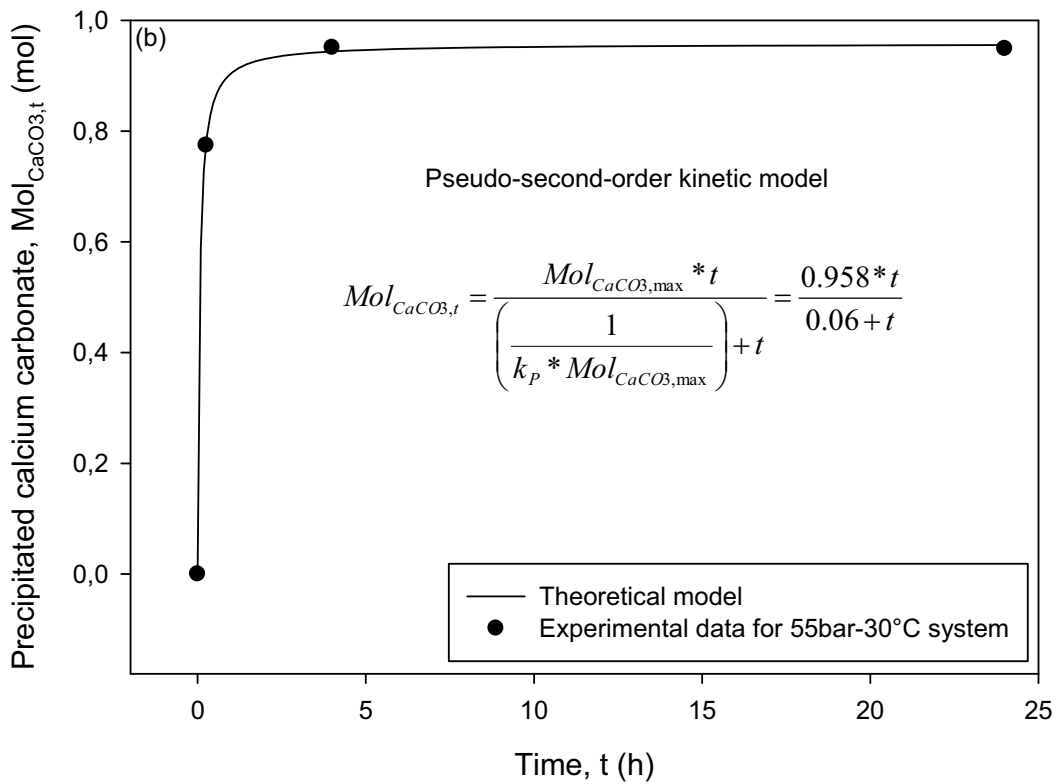
1

2

3 Figure 5. Calcite particles precipitated from $\text{CO}_2\text{-H}_2\text{O-Ca(OH)}_2$ slurry in presence of
 4 supercritical CO_2 . TEM micrographs at two different magnifications (a1, a2); SEM
 5 micrographs at two different magnifications (b1, b2).



1 a)



2 b)

3 Figure 6. Fitting of kinetic experimental data on the calcium carbonate precipitation (a) for
4 “90bar-90°C” and (b) “55bar-30°C” systems.